

Noninvasive imaging of internal muscle activities from multi-channel surface EMG recordings

Yingchun Zhang, *Senior Member, IEEE*

Abstract— Surface Electromyogram (sEMG) technology provides a non-invasive way for rapid monitoring muscle activities, but its poor spatial resolution and specificity limit its application in clinic. To overcome these limitations, a noninvasive muscle activity imaging (MAI) approach has been developed and used to reconstruct internal muscle activities from multi-channel sEMG recordings. A realistic geometric hand model is developed from high-resolution MR images and a distributed bioelectric dipole source model is employed to describe the internal muscle activity space of the muscles. The finite element method and weighted minimum norm method are utilized solve the forward and inverse problems respectively involved in the proposed MAI technique. A series of computer simulations was conducted to test the performance of the proposed MAI approach. Results show that reconstruction results achieved by the MAI technique indeed provide us more detailed and dynamic information of internal muscle activities, which enhance our understanding of the mechanisms underlying the surface EMG recordings.

I. INTRODUCTION

Muscle activity monitoring is frequently required for diagnosing neuromuscular diseases and learning the mechanisms of neuromuscular system. Intramuscular needle EMG (iEMG) provides a way for monitoring the activities of motor units invasively and has been used for both neuromuscular research and clinical application [1-3]. Since iEMG is an invasive painful procedure which requires high clinical skills [2] and sometimes even considered as interferes for muscle activity investigation [4], it's not recommended in many circumstances for neither research nor clinical application.

Surface Electromyogram (sEMG) technology provides a non-invasive way for rapid monitoring muscle activities [5]. Different from iEMG which uses needle electrode to acquire the muscle activities near the needle tip, SEMG signal is usually using multichannel surface electrodes to record the superimposed action potentials of many muscle fibers underneath covered skin surface which provides integral information of the activities from motor units such as the time of event or activity intensity. Since surface EMG signal is composed of the superimposed action potentials of many muscle fibers and is the general picture of muscle activation as opposed to the activity of only a few fibers as observed using

an inserted needle electrode in intramuscular EMG [6], it has limitation in spatial resolution and specificity limits its application in clinic [7-8]. To overcome this limitation, a muscle activity imaging (MAI) technique is developed based on a realistic geometric hand model in the present study to localize and analyze single motor unit activities from high density sEMG recordings.

II. METHODOLOGY

A. Realistic geometric hand muscle model

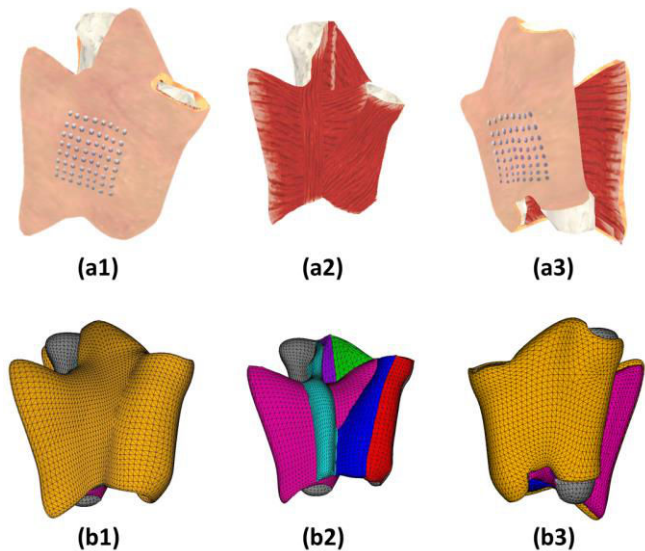


Fig. 1: Realistic geometric model and corresponding finite element model of part of right hand. Different anatomical structures are shown in different colors.

A realistic geometric model of part of the right hand (Fig. 1) is developed for the present study from the high-resolution MR images by using a subject-specific computational modeling approach [9]. The model includes the skin, fat, bones, the adductor pollicis brevis, the abductor pollicis brevis (APB), the flexor pollicis brevis, the first dorsal interosseous (FDI), and the first lumbrical muscles. The entire model consists of 98,368 tetrahedron elements and 20,000 nodes. The conductivity value of 2000 $\Omega\cdot\text{cm}$, 225 $\Omega\cdot\text{cm}$ and 2000 $\Omega\cdot\text{cm}$ were set to the bones, muscles and fat tissue respectively in the model [10].

B. Distributed dipole source model

The APB muscles are utilized as the active muscle groups in the present study. The 3-dimensional (3D) internal muscle activity space is described using a distributed dipole source space model, in which we assume that the current dipoles are evenly distributed over a fixed lattice covering the 3D APB muscles [11-12]. A total number of 3323 electrical current dipoles are evenly placed in the APB muscles with dipole

*Research supported in part by NIH K99DK082644 and the University of Houston.

Yingchun Zhang is with the Department of Biomedical Engineering, University of Houston, Houston, TX 77204 USA. (phone: 713-743-6127 fax: 713-743-0226; e-mail: yzhang94@uh.edu).

length and dipole distance both set as 1mm, and the direction of dipole moment is fixed along the muscle fiber direction for each dipole. A total number of 64 (8×8) surface electrodes are assumed over the skin for monitoring muscle activities in the computer simulation, as shown in Fig. 1(a1) and (a3).

C. Forward Solution

The forward problem can be stated by Poisson's equation which is defined on the volume conductor [13].

$$\nabla \cdot (\sigma \nabla \phi) = -\sum_{\Omega} I_s \quad \text{in } \Omega \quad (1)$$

and the Neumann boundary conditions on the scalp S

$$\sigma(\nabla \phi) \cdot n = 0 \quad \text{on S} \quad (2)$$

where σ is the conductivity tensor, n is the outward unit normal to the scalp S, and I_s the volume current densities due to the presence of current sources. The unknown ϕ is the electrical potential generated by the current sources.

A finite element solver which has been previously validated [13] is employed to calculate the electrical field within the 3D space of the hand model. Equation (1) can be formulated in a matrix form as follows and the detailed derivation can be found in our previous report [13].

$$K \cdot \Phi = G \quad (3)$$

where K is the stiffness matrix which incorporates the volume conductor model information, e.g. geometry and conductivity, Φ is the potential vector on the FE nodes, and G is the load matrix due to the internal muscle activities.

D. Inverse Solution

The relationship between the distributed dipole sources and the surface measurements can be described as

$$\Phi(t) = A * J(t) \quad (4)$$

where $\Phi(t)$ is a M×1 vector containing the surface EMG measurements at time instant t , and M is the number of recording sites. $J(t)$ is a N×1 vector containing dipole current densities at N grid points in the muscle activity source space at time instant t . A is a M×N transfer matrix relating the dipole current densities and the surface EMG signals.

Weighted Minimum Norm (WMN) method is a widely used regulation for solving ill-posed inverse problems in source localization or imaging technologies. In a model described by function (4), the WMN regulation can be used to obtain the unique solution for inverse problem by

$$\text{minimizing } \Delta = \|\Phi - AJ\|_2^2 + \lambda \|WJ\|_2^2 \quad (5)$$

where $\|\Phi - AJ\|_2^2$ is the error term in the least-squares sense, and $\lambda \|WJ\|_2^2$ is the total energy of solutions in which W is the weight matrix calculated from A and accounts for the undesired depth dependence in this model, λ is a regularization parameter determined by using the L-curve method [10].

C. Computer Simulation

The APB muscles were considered as the active muscle groups in the present computer simulation study as an example. The depolarized zone (muscle activity zone) with

the length of 4 mm was assumed for the simulated muscle activities and around 300 evenly distributed current density sources were used to model the muscle activity zone [10]. The muscle activity zone was generated in the middle of the muscle fiber groups and was assumed to propagate along the muscle fibers to the two ends. Surface EMG measurements were simulated by calculating the electrical potentials at each recording site generated by internal activating dipoles at each time instant. The simulated sEMG measurements at the sites of the 64 surface EMG electrodes were used to reconstruct the internal muscle activities by using the MAI approach.

III. RESULTS

A series of computer simulations was conducted to test the performance of the proposed MAI approach. Twelve times instants were simulated in the present computer simulations which allows the muscle activities propagate from the middle of a muscle fiber to the two ends, as shown in red dots in Fig. 2 (a1)-(a12). The simulated sEMG recordings generated by the internal muscle activities at different time instants were calculated by using the finite element method based on the realistic geometric hand model, as shown in Fig. 2 (b1)-(b12). The reconstructed muscle activities achieved from the simulated sEMG recordings by using the MAI approach were shown in green dots in Fig. 2 (c1)-(c12).

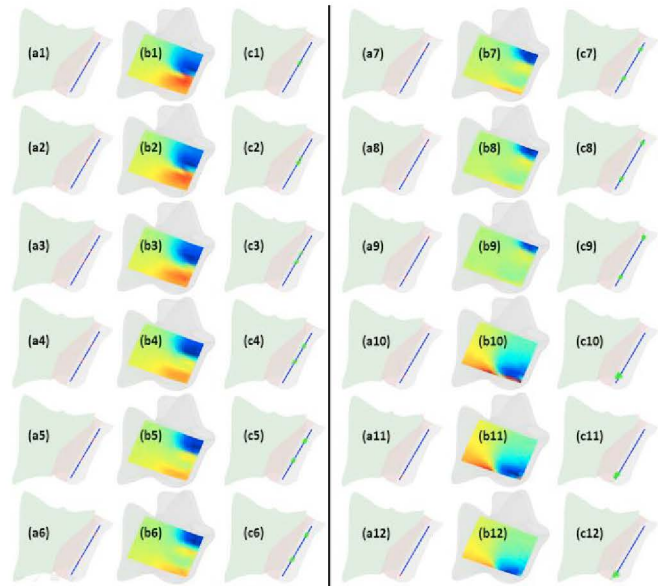


Fig. 2: The MAI imaging results of the propagating muscle activity zones. (a1)-(a12) show real locations of the propagating muscle activity zones, the assumed active muscle fiber group is shown in blue color and muscle activity zones are shown in red color. (b1)-(b12) show the skin surface EMG mapping generated by the propagating muscle activity zones, (c1)-(c12) show the reconstructed muscle activity zones in green color.

The real muscle activities, simulated surface EMG mappings and reconstructed muscle activities were enlarged and shown in Fig. 3 to better illustrate the MAI results.

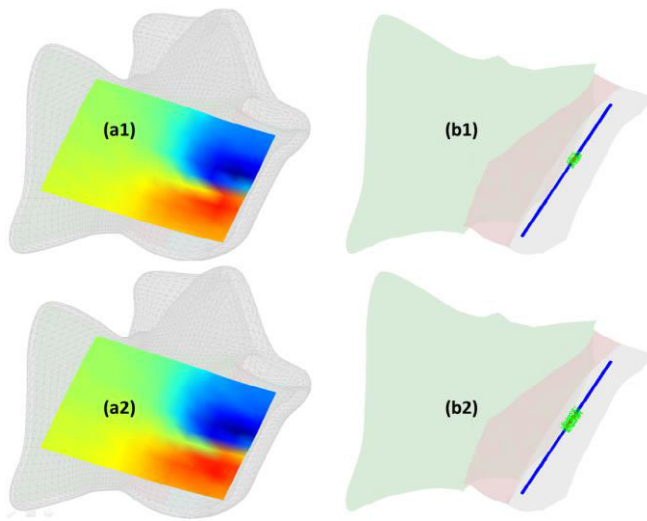


Fig. 3: Enlarged figures shows the MAI results achieved at the first two time instants. (a1) and (a2) show the simulated surface EMG mappings at the first two time instants, (b1) and (b2) show the real internal muscle activities (red dots) and the reconstructed internal muscle activities (green dots).

IV. DISCUSSION

Preliminary results demonstrate the feasibility of utilizing the proposed MAI approach to accurately reconstruct internal muscle activities from noninvasive surface EMG recordings. As we can see from Fig. 2, when internal muscle activities propagate from the middle of a muscle fiber to the two ends, their locations at different time instants cannot be captured from the surface EMG signals or mappings, even with multi-channel or high-density surface EMG recordings. With the help of the proposed MAI approach, the internal muscle activities can be accurately reconstructed in the 3D space of the muscles. This benefit was better demonstrated in Fig. 3. The simulated surface EMG mappings at the first 2 time instants are very similar in terms of pattern and magnitude, and we cannot really tell the difference visually, but from the reconstructed muscle actives, we can clearly see the muscle activities at the 2nd time instant are larger in size than them at the 1 time instant.

Since the 3D current density source model is employed in the MAI technique and the current density sources are evenly distributed in the 3D muscle space, each current density source stands for a certain amount of muscle volume. Therefore, the volume of the internal activity zones can be calculated by counting the number of current density sources reconstructed by the MAI approach. As an example present in Fig. 3, we can relatively estimate the volume of the internal muscle zones with different length by using the MAI approach although their surface EMG mappings do not tell us any remarkable difference.

The capability of localizing and imaging internal activities in muscle groups provide by the proposed MAI approach can potentially help us better estimate crosstalk among multiple muscle groups as well as to localize innervation zones of motor points where motor branches enter the muscle belly for toxin injection planning in treating patients with focal spasticity.

ACKNOWLEDGMENT

This work was supported in part by NIH K99DK082644 and the University of Houston.

REFERENCES

- [1] E. Stålberg, "Single fibre electromyography," *Trends in Neurosciences*, 2: 185 - 188, 1979.
- [2] J. R. Daube and D. I. Rubin, "Needle electromyography," *Muscle & Nerve*, 39: 244 - 270, 2009.
- [3] R. L. Barbano, "Needle EMG guidance is useful," *Muscle & nerve*, 24: 1567 - 1568, 2001.
- [4] K. Akaboshi, Y. Masakado and N. Chino, "Quantitative EMG and motor unit recruitment threshold using a concentric needle with quadrifilar electrode," *Muscle & nerve*, 23: 361 - 367, 2000.
- [5] M. J. Zwarts and D. F. Stegeman, "Multichannel surface EMG: basic aspects and clinical utility," *Muscle & nerve*, 28: 1 - 17, 2003.
- [6] G. Drost, D. F. Stegeman, B. G. van Engelen, and M. J. Zwarts, "Clinical applications of high-density surface EMG: A systematic review," *J. Electromyogr. Kinesiol.*, 16: 586 - 602, 2006.
- [7] G. Rau, C. Disselhorst-Klug, "Principles of high-spatial-resolution surface EMG (HSR-EMG): single motor unit detection and application in the diagnosis of neuromuscular disorders," *J. Electromyogr. Kinesiol.*, 7: 233 - 239, 1997.
- [8] G. Drost, D. F. Stegeman, B. G. van Engelen, and M. J. Zwarts, "Clinical applications of high-density surface EMG: A systematic review," *J. Electromyogr. Kinesiol.*, 16: 586-602, 2006.
- [9] Y. Zhang, R.M. Sweet, G.J. Metzger, D.M. Burke, A.G. Erdman, and G.W. Timm, "Advanced Finite Element Mesh Model of Female SUI Research During Physical and Daily Activities", *Studies in Health Technology and Informatics*. 142: 447-452. 2009.
- [10] Y. Zhang, D. Wang and G. W. Timm, "A three-dimensional muscle activity imaging technique for assessing pelvic muscle function," *Inverse Problems*, 26, 2010.
- [11] Y. Zhang, L. Ding, W. van Drongelen, K. Hecox, D. Frim, and B. He, "A Cortical Potential Imaging Study from Simultaneous Extra- and Intra-cranial Electrical Recordings by Means of the Finite Element Method," *Neuroimage*, 31: 1513-1524, 2006.
- [12] Y. Zhang, W. van Drongelen, M. Kohrman, and B. He, "Three-dimensional brain current source reconstruction from intra-cranial ECoG recordings," *Neuroimage*, 42: 683-695, 2008.
- [13] Y. Zhang, S. Zhu, and B. He, "A Second-Order Finite Element Algorithm for Solving the Three-Dimensional EEG Forward Problem", *Physics in Medicine and Biology*. 49:2975-2987. 2004.